Reentrant transition enthalpies of liquid crystals: The frustrated spin-gas model and experiments

J. O. Indekeu
Department of Physics, Massachusetts Institute of Technology, Cambridge, Massachusetts 02139
and Laboratorium voor Technische Natucerkunde, Technische Universiteit Delft, Lorentzweg 1, NL-2628 CJ Delft, The Netherlands

A. Nihat Berker
Department of Physics, Massachusetts Institute of Technology, Cambridge, Massachusetts 02139

C. Chiang* and C. W. Garland
Department of Chemistry, Massachusetts Institute of Technology, Cambridge, Massachusetts 02139
(Received 12 June 1986)

Specific-heat—versus—temperature curves are calculated across the reentrant (N-A_d-N-A_1) phase diagram of liquid crystals, using the microscopic "spin-gas" model. The transition enthalpies are found to be much weaker on each side of the partial bilayer smectic phase (A_d) than at the onset of the monolayer smectic phase (A_1). This qualitative difference, which agrees with experimental results obtained on octyloxybenzoyloxycyanostilbene (T8), is readily explained by the dipolar frustration reentrance mechanism of our model.

I. INTRODUCTION

As temperature is lowered, certain liquid crystals exhibit nematic (N), partial bilayer smectic (A_d), reentrant nematic (N), and monolayer smectic (A_1) phases. This interesting ordering-disordering sequence was discovered experimentally[1,2] Subsequently, it was reproduced by a microscopic theory[3,4] invoking the possible dipolar frustration of the molecules in these systems: Dipolar interactions, under the molecular close-packing conditions of these liquid crystals, may or may not be frustrated, depending on the positional fluctuations. The theory thus includes the coupled degrees of freedom of dipolar orientations and molecular positions. The upshot is that, when, in the plane normal to the average molecular axis, frustration is (is not) lifted by the positional fluctuations normal to the plane, the smectic (nematic) phase is realized.[5] These molecular positional fluctuations normal to the plane are called permeation fluctuations.

Recent calculations[4] with this "frustrated spin-gas model" have also reproduced the remarkable experimental sequence[6,7] of N-A_d-N-A_d-N-A_1, as well as the stringent condition on the length of the molecular tail necessary for this quadruple reentrance. These calculations have also yielded relative layer thicknesses for the distinct smectic phases in satisfactory agreement with experiment.

In the present paper we report calculations of the temperature dependence of the specific heat, obtained with the frustrated spin-gas model, for the sequence N-A_d-N-A_1. We find a qualitative difference between the transition enthalpies at the onsets of the smectic A_d and A_1 phases, in agreement with our distinct microscopic pictures of these smectic phases. The theoretical results are compared with experimental measurements of the heat capacity of octyloxybenzoyloxycyanostilbene (T8). A general agreement is seen between theory and experiment.

II. THEORETICAL METHOD

We first summarize the theoretical method introduced and used in Refs. 3 and 4. The microscopic pair potential through which the molecules interact is taken to be

$$V(\mathbf{r}_1,\hat{\mathbf{s}}_1,\mathbf{r}_2,\hat{\mathbf{s}}_2)=\frac{A\hat{\mathbf{s}}_1\cdot\hat{\mathbf{s}}_2-3B(\hat{\mathbf{s}}_1\cdot\hat{\mathbf{r}}_{12})(\hat{\mathbf{s}}_2\cdot\hat{\mathbf{r}}_{12})}{|\mathbf{r}_{12}|^3}\ , \tag{1}$$

where $\mathbf{r}_i$ is the position of the dipolar head of molecule i, $\hat{\mathbf{s}}_i=\pm\hat{\mathbf{z}}$ is the unit vector describing the dipolar orientation along the molecular axis z, and $\mathbf{r}_{12}=\mathbf{r}_1-\mathbf{r}_2$ and $\hat{\mathbf{r}}_{12}=\mathbf{r}_{12}/|\mathbf{r}_{12}|$. A purely dipolar interaction, $A=B$, is modified by tail-tail interactions, $A>B$ reflecting net steric hindrance and $A<B$ reflecting net van der Waals attraction. The important positional fluctuations for the reentrant systems were found to be permeation fluctuations, occurring along the z direction, which is parallel to the average molecular axis and normal to the smectic layers possible under the present model. Because of the unsmooth molecular architecture, for a given molecule, a nearest-neighbor molecule has n positions of preferred relative permeation. These "notches" are taken to be separated by l/n, where l is the effective molecular length.[8] For more information on the construction of this microscopic model and on its approximate treatment (next paragraph), the reader is referred to the previous papers.[3,4]

A special prefacing transformation is used to evaluate the effect of the positional fluctuations on the dipole-dipole interactions. In a finite-cluster approximation, a triplet of nearest-neighbor dipoles is considered. With one dipole fixed (e.g., in notch 5 for $n=9$), the partition function is summed over the n^2 permeational configurations of the two other dipoles (see Fig. 1). The outcome is a triplet spin Hamiltonian, into which have been projected the average strongest, intermediate, and weakest antiferroelectric couplings:

$$\exp(\mathscr{H}_{123}+G)\equiv\exp(K_S s_1 s_2+K_I s_2 s_3+K_W s_3 s_1+G)$$
$$=\sum_{\mathbf{r}_{2,3}}\exp[-\beta V(\mathbf{r}_1,\hat{\mathbf{s}}_1,\mathbf{r}_2,\hat{\mathbf{s}}_2)-\beta V(\mathbf{r}_2,\hat{\mathbf{s}}_2,\mathbf{r}_3,\hat{\mathbf{s}}_3)-\beta V(\mathbf{r}_3,\hat{\mathbf{s}}_3,\mathbf{r}_1,\hat{\mathbf{s}}_1)]\ , \tag{2}$$

where the three molecules are labeled 1, 2, and 3 such that (12), (23), and (31) always span the strongest, intermediate, and weakest antiferroelectric couplings, respectively. In Eq. (2), G is the free energy contribution of the degrees of freedom summed over in the prefacing transformation. The result is a distorted triangle of Ising spins. Houtappel's criticality condition[9] is invoked to locate the nematic-smectic phase boundaries. Figure 2 gives such a phase diagram for $n=9$ and $B/A=2$. The ratio of the lateral separation to the molecular length, a/l, is a (dimensionless) measure of inverse pressure, whereas l^3kT/A is the dimensionless temperature. The doubly reentrant sequence, nematic→ smectic-A_d→reentrant-nematic→smectic-A_1 as temperature is lowered, is thus encountered.[10]

This procedure is now extended to the calculation of specific heat. After the prefacing transformation [Eq. (2)], the free energy per molecule can be expressed as

$$f=G+\ln\lambda(K_S,K_I,K_W)\ , \tag{3}$$

with

$$\ln\lambda(K_S,K_I,K_W)=\lim_{N\to\infty}\left[\frac{1}{N}\ln\sum_{\{s\}}\exp\left[\sum_{\langle ijk\rangle}\mathscr{H}_{ijk}\right]\right]\ ,$$

where the last sum is over the N up-triangles formed in a plane of N spins. (Recall here that the premise of the employed prefacing transformation is that the original spin system subject to annealed positional disorder can be represented well by a lattice statically and uniformly distorted in a manner determined by the variance of the original disorder. The mapping is conducted accordingly.) The specific heat per molecule at constant pressure (a/l) is then given by

$$C=\frac{\partial}{\partial T}kT^2\frac{\partial}{\partial T}f\ , \tag{4}$$

which is evaluated with the chain rule, requiring the first and second temperature derivatives of G and K_α. These are extracted from the prefacing transformation, Eq. (2). For the function $\lambda(K_S,K_I,K_W)$, Houtappel's exact expression[9] for the distorted triangular Ising model is used:

$$8\pi^2\ln(\lambda/2)=\int_0^{2\pi}dw_1\int_0^{2\pi}dw_2\ln[\cosh(2K_S)\cosh(2K_I)\cosh(2K_W)+\sinh(2K_S)\sinh(2K_I)\sinh(2K_W)$$
$$-\sinh(2K_S)\cos w_1-\sinh(2K_I)\cos w_2-\sinh(2K_W)\cos(w_1+w_2)]\ . \tag{5}$$

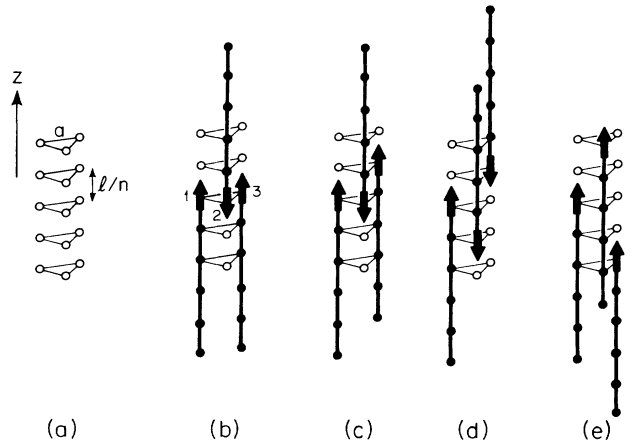

FIG. 1. Examples of configurations of a triplet of molecules. (a) The atomic permeation positions of the dipole heads. (b) A frustrated configuration: a zero net force is felt by either of dipoles 1 and 3. (c) Another frustrated configuration: a zero net force is felt by dipole 3. Configurations (b) and (c) are thus not conducive to layering. On the other hand, (d) and (e) are configurations in which frustration is relieved by permeation, respectively conducive to interdigitated, partial bilayer (A_d) and monolayer (A_1) smectic layering.

We are interested in the relative magnitudes of the specific-heat signals at the different phase transitions, which are strongly affected by the functions $G(T)$ and $K_\alpha(T)$ of the prefacing transformation. These magnitudes are nonuniversal properties distinctly applicable to each phase transition under consideration.

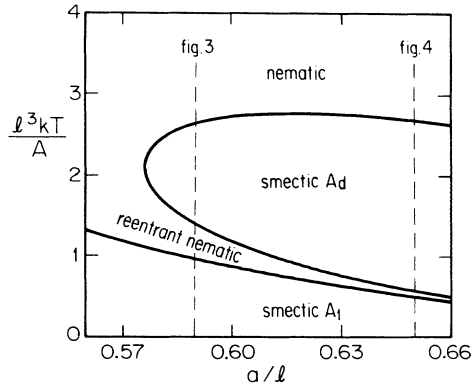

FIG. 2. Doubly reentrant phase diagram, obtained with $n=9$ and $B/A=2$ (net tail-tail attraction). The dashed lines only mark the paths along which specific heats were computed for display in Figs. 3 and 4.

III. THEORETICAL RESULTS

Figures 3 and 4 show the calculated specific heat versus temperature, along the two paths ($a/l=0.59$ and 0.65) indicated on the phase diagram of Fig. 2. From Fig. 3 it is clear that the "transition enthalpy", i.e., the area under the specific-heat peak, is much larger for the smectic-A_1—to—reentrant-nematic transition than for the reentrant-nematic—to—smectic-A_d transition. In Fig. 4, where the reentrant-nematic range is narrower, this still appears to be true, to the extent that the two peaks can be resolved. The insets in Figs. 3 and 4 show specific heats across the smectic-A_d—to—nematic transition. It is seen that these transition enthalpies are comparable in magnitude to that of the reentrant-nematic—to—smectic-A_d transition.

The qualitative difference between the N-A_1 and N-A_d transition enthalpies is obtained in our theory irrespective of variations of input model parameters. In fact, this difference can be microscopically understood in terms of the smectic ordering mechanisms of our model. The smectic-A_d phase (interdigitated, partial bilayer) has dominant antiferroelectric nearest-neighbor couplings (see Table I of Ref. 4). Frustration is lifted by the differing strengths of the local antiferroelectric couplings. Still, many of the couplings are not satisfied in the ordered phase. Only a subset of the molecules participates in the smectic order, by forming a "polymer" defining the layer, in the extensive presence of dimers and other n-mers which maintain a nematic background. Thus, the ordering is tenuous, and the associated enthalpy understandably small. By contrast, the smectic-A_1 phase (monolayer) has dominant ferroelectric couplings (Table I, Ref. 4), which do not compete with each other. Upon ordering, all such couplings are satisfied, hence the large transition enthalpy.

Before proceeding with the experimental comparison, one caveat is in order. Our specific-heat curves have been calculated at constant a/l, the ratio of the lateral molecular separation to the molecular length. This lateral separation a is expected to be a monotonic function of pressure. It is also clearly linked to the in-plane density. The bulk density, however, can vary independently of a, via changes in the layer thickness. In sum, it is beyond the scope of the present calculation to distinguish between C_P and C_V. At the ordinary liquid-gas critical point, C_P and C_V have quite different singularities because the density is the order parameter. On the other hand, at the N-A transition lines of liquid crystals, because the density is not the order parameter, the difference between C_P and C_V is quantitative rather than qualitative. This justifies comparing the qualitative findings of our theory and our experiments.

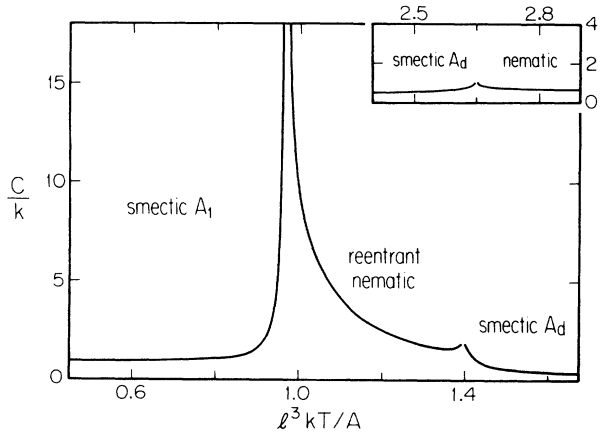

FIG. 3. Specific heat per molecule vs temperature along the path $a/l=0.59$ (see Fig. 2). The inset, on the same scale, shows the result for the high-temperature N-A_d transition.

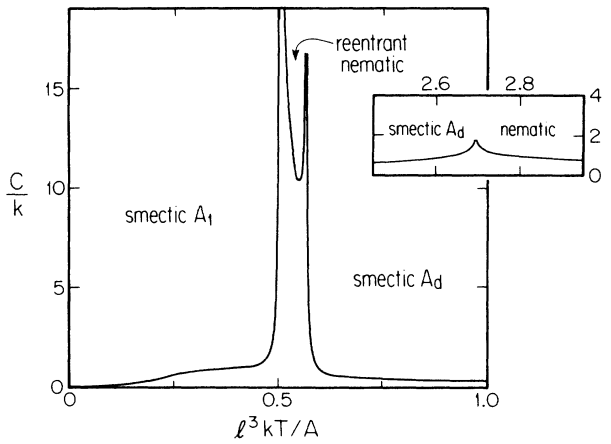

FIG. 4. Specific heat per molecule vs temperature along the path $a/l=0.65$ (see Fig. 2). The inset, on the same scale, shows the result for the high-temperature N-A_d transition.

IV. EXPERIMENTS

The type of reentrant phase diagram shown in Fig. 2 is well realized experimentally for the alkoxybenzoyloxycyanostilbenes T7, T8, T9, and their mixtures.[7] Thus, we have carried out a measurement of the specific heat C_P of octyloxybenzoyloxycyanostilbene (T8) in order to provide an experimental test of our theoretical predictions. These measurements were made with an ac calorimetric technique described elsewhere.[11] The observed values C_P(obs) correspond to the heat capacity of a sealed silver cell containing 72.1 mg of T8. Values of the specific heat were then obtained from

$$C_P=[C_P(\text{obs})-C_P(\text{empty})]/0.0721\ , \tag{6}$$

where C_P(empty) is the measured heat capacity of the empty cell, which is roughly one-half C_P(obs).

The experimental specific heat of T8 over the range 335 to 415 K is shown in Fig. 5. This overview, obtained from a fairly rapid cooling scan (2 to 8 K/h), shows two rather small heat-capacity peaks associated with the A_d-N and N-A_1 transitions at 410.52 and 367.41 K, respectively. Note also that the noncritical background variation in C_P is linear as expected. Detailed measurements were made in the vicinity of these two transitions, and the resulting excess specific heats $\Delta C_P=C_P-C_P$ (background) are shown in Fig. 6. In order to facilitate comparison with the theoretical results, the excess molar specific heats

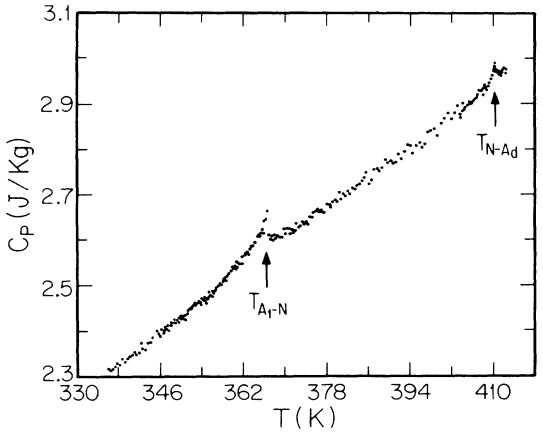

FIG. 5. Specific heat per gram vs temperature for T8.

$\Delta\tilde{C}_P$ are given in the dimensionless form $\Delta\tilde{C}_P/R$.

The N-A_1 specific heat peak in Fig. 6(a) is small but quite well characterized, since the transition temperature $T_c(N\text{-}A_1)$ was stable. The excess A_d-N specific heat is not quite as well characterized, since the peak is very small [the maximum value of $\Delta C_P(A_d\text{-}N)$ represented only 0.8% of C_P(obs)] and $T_c(A_d\text{-}N)$ drifted by ~ 25 mK/h. However, Fig. 6(b) shows reasonable agreement in the shape and size of the peak obtained on a cooling run and a subsequent warming run.

The transition enthalpy δH for a second-order phase transition is defined as the integrated area under the excess specific-heat curve, i.e., $\delta H = \int \Delta\tilde{C}_P\, dT$. For T8, we find $\delta H(N\text{-}A_1) = 97$ J/mol and $\delta H(A_d\text{-}N) = 30 \pm 10$ J/mol. Thus, a major qualitative feature of our theory—the prediction that $\delta H(N\text{-}A_1)$ should be significantly larger than $\delta H(A_d\text{-}N)$—is in complete agreement with the experimental results on T8. It should, however, be noted that the temperature range and asymmetry of the experimental N-A_1 excess specific-heat peak shown in Fig. 6(a) (which are consistent with N-A_1 peaks in liquid crystals with no reentrance[12]) do not agree well with these features of our theoretical calculation.

ac calorimeter measurements were not made in the vicinity of the upper N-A_d transition, which occurs at ~ 521.7 K for T8.[13] However, differential-scanning-calorimetry (DSC) measurements on T8 and on mixtures of T7 and T8 show that the transition enthalpy at the upper N-A_d transition is very similar to that at the lower A_d-N transition.[13] Thus, this feature of our theoretical

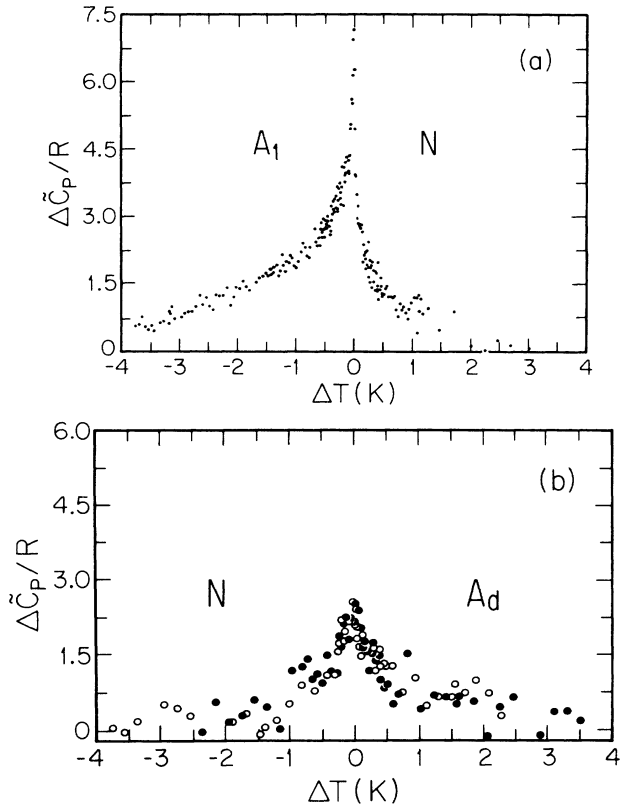

FIG. 6. Excess specific heat per mole of T8 associated with (a) the reentrant-nematic—smectic-A_1 transition, and (b) the smectic-A_d—reentrant-nematic transition, vs $\Delta T \equiv T - T_c$, where $T_c(N\text{-}A_1) = 367.41$ K and $T_c(A_d\text{-}N) = 410.52$ K. In (b), a cooling run and a subsequent heating run are shown, respectively, with solid and open circles.

results is also in good qualitative agreement with experiment.

ACKNOWLEDGMENTS

We thank P. Das and F. Dowell for useful and enjoyable discussions. We gratefully acknowledge the Council for International Exchange of Scholars, the Belgian National Fund for Scientific Research, and the Dutch Stichting F.O.M. for support for J.O.I., and the Alfred P. Sloan Foundation for support for A.N.B. This research was supported by the National Science Foundation under Grant No. DMR-84-18718.

*Current address: Intel Corporation, Livermore, California 94550.

[1]P. E. Cladis, Phys. Rev. Lett. **35**, 48 (1975).

[2]F. Hardouin and A. M. Levelut, J. Phys. (Paris) **41**, 41 (1980).

[3]A. N. Berker and J. S. Walker, Phys. Rev. Lett. **47**, 1469 (1981).

[4]J. O. Indekeu and A. N. Berker, Phys. Rev. A **33**, 1158 (1986). See also J. O. Indekeu and A. N. Berker, Physica (Utrecht) **140A**, 368 (1986); A. N. Berker and J. O. Indekeu, in *Incommensurability in Crystals, Liquid Crystals, and Quasi-Crystals,* edited by J. F. Scott (Plenum, New York, 1987).

[5]For another microscopic mechanism for liquid crystal reentrance, see F. Dowell, Phys. Rev. A **28**, 3526 (1983); **31**, 2464 (1985); **31**, 3214 (1985).

[6]N. H. Tinh, F. Hardouin, and C. Destrade, J. Phys. (Paris) **43**, 1127 (1982).

[7]F. Hardouin, A. M. Levelut, M. F. Achard, and G. Sigaud, J. Chim. Phys. **80**, 53 (1983).

[8]In addition to this "atomic permeation," a weaker "librational permeation" occurs on a subatomic length scale (see Refs. 3 and 4). This has been omitted in the current calculation.

[9]R. F. M. Houtappel, Physica (Utrecht) **16**, 425 (1950).

[10]This reentrance sequence was experimentally first reported in Ref. 2. The phase diagram was derived in Ref. 3.

[11]C. W. Garland, Thermochim. Acta **88**, 127 (1985), and references therein.

[12]C. Chiang and C. W. Garland, Mol. Cryst. Liq. Cryst. **122**, 25 (1985).

[13]N. H. Tinh, G. Sigaud, M. F. Achard, H. Gasparoux, and F. Hardouin, in *Advances in Liquid Crystal Research and Applications,* edited by L. Bata (Pergamon, Oxford, 1980), p. 147.